Title: Decoupling the effects of deforestation and climate variability in the Tapajós river basin in the Brazilian Amazon

Authors and affiliations

Mauricio E. Arias[1]*, Eunjee Lee[2], Fabio Farinosi[3], Fabio F. Pereira[4], and Paul R. Moorcroft[5]

[1] Department of Civil and Environmental Engineering, University of South Florida, Tampa, FL, USA.

[2] Global Modeling and Assimilation Office, NASA Goddard Earth Sciences Technology and Research, Universities Space Research Association, Columbia, MD, USA.

[3] European Commission, DG Joint Research Centre, Ispra, Italy.

[4] Department of Renewable Energy Engineering, Federal University of Alagoas, Maceió, AL, Brazil.

[5] Department of Organismic and Evolutionary Biology, Harvard University, Cambridge, MA, USA.

*** Corresponding author**: Department of Civil and Environmental Engineering, University of South Florida, 4202 E. Fowler Ave, Tampa, FL 32620, USA. Tel. +1 (813) 974-5593, Email: mearias@usf.edu.

This article has been accepted for publication and undergone full peer review but has not been through the copyediting, typesetting, pagination and proofreading process which may lead to differences between this version and the Version of Record. Please cite this article as doi: 10.1002/hyp.11517

Running head: Decoupling effects of deforestation and climate variability in the Tapajós river basin

Keywords: Tapajós River; Southeastern Amazonia; Ecosystem Demography Model; land cover dynamics.

Abstract

Tropical river basins are experiencing major hydrological alterations as a result of climate variability and deforestation. These drivers of flow changes are often difficult to isolate in large basins based on either observations or experiments; however, combining these methods with numerical models can help identify the contribution of climate and deforestation to hydrological alterations. This paper presents a study carried out in the Tapajós River (Brazil), a 477,000 km^2 basin in Southeastern Amazonia, in which we analyzed the role of annual land cover change on daily river flows. Analysis of observed spatial and temporal trends in rainfall, forest cover, and river flow metrics for 1976 to 2008 indicates a significant shortening of the wet season and reduction in river flows through most of the basin despite no significant trend in annual precipitation. Coincident with seasonal trends over the past four decades, over 35% of the original forest (140,000 out of 400,000 km^2) was cleared. In order to determine the effects of land clearing and rainfall variability to trends in river flows, we conducted hindcast simulations with ED2+R, a terrestrial biosphere model incorporating fine scale ecosystem heterogeneity arising from annual land-use change, and linked to a flow routing scheme. The simulations indicated basin-wide increases in dry season flows caused by land cover transitions beginning in the early 1990s when forest cover dropped to 80% of its original extent. Simulations of historical potential vegetation in the absence of land cover transitions indicate that reduction in rainfall during the dry season (mean of -9 mm per month) would have had an opposite and larger magnitude effect than deforestation

(maximum of +4 mm month per month), leading to the overall net negative trend in river flows. In light of the expected increase in future climate variability and water infrastructure development in the Amazon and other tropical basins, this study presents an approach for analyzing how multiple drivers of change are altering regional hydrology and water resources management.

1. Introduction

Understanding the interplay between climate variability and land cover is fundamental to the conservation and sustainable management of tropical river basins, where forests play an important role in regional water and carbon cycles, and are major reservoirs of biological diversity (Bonell and Bruijnzeel, 2005; Lewis et al., 2015). This is particularly true in the Amazon, the world's largest river basin and largest remaining tropical forest, where deforestation and climate variability threaten to cause major environmental and hydrological alterations at regional, continental, and global scales (Coe et al., 2013; Davidson et al., 2012; Malhi et al., 2008).

The interactions among climate, forest cover, and the water cycle have been well studied in the Amazon and other tropical regions (Coe et al., 2013, 2009; Rodriguez et al., 2010; Spracklen et al., 2012; Swann et al., 2015), but the specific roles of deforestation and climate variability in contemporary regional trends of river discharge have been relatively understudied. Field observations in farmed watersheds have revealed that clearing of tropical forests followed by cropping led to an increase in flows after a few years as a result of changes to infiltration capacity of soils and vegetation transpiration (Hayhoe et al., 2011; Neill et al., 2013). Moreover, an analysis of multi-decadal records –in the absence of annual rainfall trends– supports that a continuous increase of discharge may have occurred with gradual deforestation (Costa et al., 2003). However, seasonal patterns of rainfall have also

changed markedly across the Amazon in recent decades, primarily with a negative trend in the dry and early rainy seasons (June-November; Espinoza Villar et al., 2009b). Recent findings suggest that regional trends in contemporary rainfall have been primarily linked to inter-annual and decadal climate oscillations (Espinoza Villar et al., 2009b; Marengo, 2004), but more localized studies found that forest cover could also have played a role in the timing and frequency of rainfall (Butt et al., 2011; Knox et al., 2010).

Overall, despite significant trends in the atmospheric component of the water cycle (Costa and Foley, 1997; Gloor et al., 2013) and deforestation (Leite et al., 2010; Morton et al., 2006; Soares-Filho et al., 2006), no significant trends have been observed in the discharge of the Amazon and other meso-scale tropical basins (Beck et al., 2013; Espinoza Villar et al., 2009a; Wilk et al., 2001). Moreover, there is evidence suggesting that elevated CO_2 fertilization has had little impact on the hydrological cycle of tropical forests (Yang et al., 2016). These conflicting bodies of evidence support the need for studies that decouple the effects of different drivers of hydrological change at basin and sub-basin scales where significant trends in river discharge have been observed (Costa et al., 2003; Espinoza Villar et al., 2009a).

Land surface models representing climate-ecosystem-water interactions have been primary tools to identify and quantify the impact of different drivers of environmental change on the water cycle of tropical forests. Early applications highlighted the importance of forest cover in the overall water cycle by driving evapotranspiration (Costa and Foley, 1997), which is typically expected to decrease with deforestation, thus increasing runoff (Bruijnzeel, 2004; Wohl et al., 2012). This direct effect on water discharge is clear in the tropics until deforestation reaches a tipping point at which –according to computer simulations– ET decreases so much that it could result in a negative feedback to the recycling of moisture into the atmosphere, thus decreasing rainfall(Coe et al., 2009; Van der Ent et al., 2010).Computer

simulations of direct effects of deforestation show that loss of forest cover has a net positive effect on river discharge in the Amazon and its tributaries (Coe et al., 2011, 2009; Panday et al., 2015), consistent with field observations at the plot to watershed scales. However, sub-continental scale simulations using coupled land-atmosphere models have shown that although past deforestation might not have affected basin-wide rainfall patterns (Knox et al., 2015), future extensive deforestation (ac. 30% of the Amazon forest) may lead to reductions in rainfall sufficiently large to cause negative discharge trends (Coe et al., 2009). Despite the importance of ET to the water cycle, large discrepancies among ET estimates and substantial seasonal differences have been found for several land surface models over the Amazon when compared to field (FLUXNET) measurements (Getirana et al., 2014). However, land surface models that incorporate sub-grid scale ecosystem heterogeneity and spatiotemporal dynamics arising from land-use change have been able to accurately match field ET observations (Kim et al., 2012; Longo, 2014).

In this analysis, we used the Ecosystem Demography 2 model (ED2) in combination with a flow routing scheme and multi-decadal records of river flows, precipitation and land-cover change to quantify the role that climate variability and deforestation have on river flows in large tropical rivers with observed environmental changes in recent decades. Specifically, this study addresses the three following inter-related questions:

1. What were the temporal and spatial trends in rainfall and deforestation across the basin?
2. What was the influence of rainfall variability on river flows?
3. What was the role of deforestation in explaining past flow trends?

These three questions/objectives provide the structure of the Methods and Results sections. To answer the first question, we examine patterns of rainfall, deforestation, and river flows through six sub-basins. To answer the second and third questions, the effects of

deforestation on ET and river flows –dynamically represented with annual land cover transitions– were isolated from those of rainfall via hindcast simulations with different land cover transitions using the ED2 terrestrial biosphere model with a flow routing scheme (ED2+R).

2. ED2+R model description

ED2 is a terrestrial biosphere model that describes vegetation dynamics (growth, reproduction, and mortality), and accompanying energy, carbon and water fluxes of heterogeneous and functionally diverse plant canopies as a function of climate, soils, and human disturbance characteristics (Medvigy et al., 2009; Moorcroft et al., 2001). Recently, ED2 has been used to assess the future fate of carbon fluxes in the Amazon forests (Kim et al., 2012; Levine et al., 2016; Zhang et al., 2015). ED2 represents the plant canopy structure (i.e., biomass, height, leaf area) and corresponding material fluxes in a more realistic way than conventional land surface models, which typically assume that the plant canopy within climatological grid cells is homogeneous (Longo, 2014). ED2 uses a distribution-based approach to incorporate horizontal heterogeneity in the composition and structure of vegetation heterogeneity down to the scale of approximately 10 meters. Vertical heterogeneity in composition and structure is represented explicitly with a multi-layer canopy with adaptive number of vegetation layers depending on the structural and compositional complexity of the ecosystem: in forested areas, the number of canopy layer is typically between 10-20 layers, while in agricultural areas is typically 1-2 vegetation layers. This canopy composition is represented by a system of age and size structured partial differential equations that dynamically track ecosystem composition, structure, and functioning at the sub-grid cell scale (Medvigy et al., 2009; Moorcroft et al., 2001). The ED2 model components most relevant to this paper, namely those related to land transformation and

water fluxes, are summarized below. Further details and conceptual diagrams of the ED2 model formulation can be found elsewhere (Longo, 2014; Medvigy et al., 2009; Pereira et al., 2017).

ED2 tracks horizontal ecosystem heterogeneity arising from natural and anthropogenic disturbances by calculating the rate at which transitions between different land-use states occur as function of time since last disturbance. Following the implementation of Albani et al. (2006), land-use dynamics within each grid cell are characterized in terms of the annual rate of transitions between three land use states: primary (natural) vegetation, secondary vegetation, and agricultural/cleared land. Anthropogenic land-use change processes involve transitions of land from primary vegetation to agriculture (land clearing), transitions from agriculture to secondary vegetation (land abandonment), transitions from secondary land to agriculture (secondary land clearing), and the rate of forest harvesting of primary and secondary vegetation (Albani et al., 2006). When land clearing occurs, rooting depth changes from 2~3 meters for trees to 1 meter for C_4 grasses. Land clearing also prevent the recruitment and growth of trees; however, if land abandonment occurs, then tree plant functional types (PFTs) can re-establish and growth. Land cover transitions also affects structure and composition of the plant canopy, affecting the rate of plant transpiration, and also soil water availability. Canopy-level evaporation and soil evaporation can also change, contributing to the overall change in ET arising from deforestation. Soil structural characteristics such as hydraulic conductivity and texture, however, remain constant for a given grid cell through the simulation.

ED2 computes vertically resolved energy and water budgets within the ecosystem at sub-hourly time steps for the air, soil, vegetation, and surface water for each of the tiles (sub-grid scale land areas that share a common disturbance history) within a climatological grid cell. Water flux through a soil layer k ($\dot{W}_k$) is defined as follows:

$$\dot{W}_k = \dot{L}_k - \dot{I}_k - \dot{E}_k - \dot{Q}_{sub,k} - \sum_{m=1}^{M} \dot{U}_m \quad (1)$$

where $\dot{L}_k$ is the water flux between soil layers (a total of 16 were considered), $\dot{I}_k$ is percolation from the temporary surface water, $\dot{E}_k$ is evaporation from the ground, $\dot{Q}_{sub,k}$ is subsurface runoff, and $\dot{U}$ is water uptake from vegetation layers m (m = 1,…,M). The M vegetation layers can have different physiological and biophysical properties depending on their PFT, which included in the simulations conducted are: C_4 grasses, plus early successional tropical trees, mid-successional tropical trees, late successional tropical trees (all which are C_3 plants). Surface water ($\dot{W}_s$) occurs temporarily in the model as a function of percolation into the top soil layer, evaporation, and precipitation throughfall:

$$\dot{W}_s = \dot{L}_s + \dot{I}_s - \dot{E}_s - \dot{Q}_s + \sum_{m=1}^{M} \dot{D}_m \quad (2)$$

where $\dot{L}_s$ is the percolation between ponding layers, $\dot{I}_s$ is percolation to the ground, $\dot{E}_s$ is surface water evaporation, $\dot{Q}_s$ is surface runoff, and $\dot{D}$ is canopy dripping. This last parameter is a function of the maximum water holding capacity in leaves and branches, which range from 0.05 to 0.40 kg m^{-2} (Wohlfahrt et al., 2006). Flux of water intercepted by the vegetation layers ($\dot{W}_m$) is a function of rainfall interception, canopy dripping, water uptake from soil, transpiration, and evaporation of intercepted water:

$$\dot{W}_m = \dot{P}_m - \dot{D}_m - \dot{E}_m - \dot{T}_m + \sum_{k=k_m}^{K} \dot{W}_k \quad (3)$$

Where $\dot{P}_m$ represents precipitation interception, $\dot{E}_m$ is evaporation of intercepted water, $\dot{T}_m$ is transpiration, and k_m refers to the deepest soil layer that vegetation has access to.

Evaporation and transpiration are computed separately. Evaporation from the soil, leaf surfaces, and temporary surface water are function of their moisture content, conductance, and the moisture content of the canopy air space. Transpiration is calculated using stomatal conductance via the Ball-Berry-Leuning model (Leuning, 1995), which accounts for the

effect of vapor pressure deficit and the leaf-level photosynthesis rate via the Farquhar model (Farquhar et al., 1980). The rate is further regulated by a plant's soil water availability:

$$\dot{T}_m = \dot{T}_{m,max}\beta - (1-\beta)\dot{T}_{m,min} \quad (4)$$

where $\dot{T}_{m,max}$ is the hydraulically unlimited potential transpiration, $\dot{T}_{m,min}$ is the cuticular transpiration, and β is the dimensionless scaling factor that accounts for the effect of soil moisture limitation on stomatal conductance:

$$\beta = \sum_{k=k_m}^{K} \left(1 / \left[\frac{\dot{T}_{m,max} LAI}{S_k}\right]\right) \quad (5)$$

Where *LAI* is the leaf area index and S_k is the soil moisture supply, which is the product of the soil hydraulic conductivity, volumetric soil moisture, and root biomass. For more details on the transpiration calculations, see Appendix B in Medvigy et al. (2006) and Powell (2015).

The vertical fluxes of water within each sub-grid tile are integrated up to the climatological grid cell scale (typically in the order of 1 to 10^4 km^2). All water fluxes described above are formulated in units of kg m^{-2} s^{-1}. The reader is referred to Longo (2014) and Powell (2015) for a more detailed description of the formulations implemented of these hydrological processes in ED2.

In the native ED2 formulation there are no lateral hydrological connections either within or between grid cells. In ED2+R, however, surface runoff ($\dot{Q}_s$ in equation 2) and subsurface runoff ($\dot{Q}_{sub}$ in equation 1) within each grid-cell are routed horizontally from each climatological cell to the nearest stream using a runoff and river flow routing scheme (+R) adapted from MGB-IPH (Collischonn et al., 2007). Total daily surface and subsurface runoff from ED2 are transferred to the horizontal routing scheme (+R), which partitions the total runoff volume into three linear reservoirs with different residence times (surface flow, interflow, and groundwater reservoirs), representing in this way the flow routing and delay

through grid cells. Flow through the river network is calculated following the Muskingum-Cunge method, which computes water flow and attenuation as a function of terrain elevation and channel dimensions. A detailed description of the ED2+R can be found in Pereira et al. (2017).

3. Study Site and Materials

3.1 Description of the study basin

The Tapajós is a large (476,674 km^2) basin in Southeastern Amazonia located within the Brazilian states of Amazonas, Rondônia, Pará, and Mato Grosso. Elevation in the basin ranges from nearly 800 m above sea level (asl) in the headwaters in Mato Grosso to 7 m asl at its mouth at Santarém. The Tapajós river itself has a length of nearly 1,880 km, and its two largest tributaries, the Juruena and Teles Pires, have lengths of 1,009 and 1,638 km, respectively (ANA, 2011). According to our analysis, annual rainfall ranges from 1,274 to 2,624 mm, with relatively lower precipitation in the headwaters, and higher rainfall in the lower Juruena and upper Tapajós regions (Table 1). Rainfall is seasonal, with highest monthly precipitation of 300-400 mm in December-March (wet season) and lowest monthly precipitation (less than 50mm) in June-August (dry season). The Tapajós discharges a mean daily discharge of 11,833 m^3/s, making it the fifth largest tributary in terms of flow contribution to the Amazon River (WWF/TNC, 2013).

Here, the Tapajós was divided into seven units/sub-basins with distinct hydrological conditions, recent land cover change, and sufficient river flow records to calibrate the model (Figure 1). All analyses and description of results are made with reference to these sub-basins. Discharge at Itaituba (the furthest downstream river gauging station) is assumed to represent the Tapajós basin discharge, and all basin-wide results relate to this river gauge and its contributing area.

3.2 Data sets

Data for this study came from global and regional, freely available and peer-reviewed datasets. These are summarized in Table 2. Climate, land-use, and soils data are those described in Zhang et al. (2015). Spatially distributed land-use history was prescribed from a global dataset of land-use transitions derived from historical land-use states, potential biomass density, and national wood harvest inventories (Hurtt et al., 2006). This dataset is only available up to the year 2000; land cover transitions for the remaining years of simulation were derived from an Amazon-wide deforestation (governance) scenario that resembled the legislation and enforcement measures that reduced deforestation rates in the Brazilian Amazon since the early 2000s (Soares-Filho et al., 2006). Annual deforestation rates from the latter dataset were compared against those estimated from a 1-km resolution tree cover dataset derived from the MODIS satellite sensors (MOD44b; DiMiceli et al., 2011), and overall, deforestation rates appeared to be similar, although the absolute extent of deforestation is greater in the MOD44b dataset (56% or 269,679 km^2 of the basin estimated to be forested in 2008) than in the Soares-Filho et al. (2006) governance scenario (340,000 km^2 or 70% of the basin forested in 2008).

Flow data used to study trends during 1970s-2000s and to calibrate ED2+R came from the Brazilian Water Agency (ANA) water resources information system and from the Observation Service for Geodynamical, hydrological and biogeochemical control of erosion/alteration and material transport in the Amazon, Orinoco and Congo basins (SO HYBAM). 15 river flow monitoring stations were available from the 1960s, but only a selected number of them had sufficient daily records. In order to interpolate data gaps, multivariable linear regressions for each of the seven stations listed in Table 1 were developed using daily records for years prior and after at each station, as well as same-day

records for two adjacent stations as the depending variables as explained in detail by Pereira et al. (2017):

$$Obs_y(t) = K + \beta_1 \cdot Obs_z(t) + \beta_2 \cdot Obs_q(t) + \beta_3 \cdot Obs_y(t-365) + \beta_4 \cdot Obs_y(t+365) \quad (4)$$

Where *z*, *y* and *q* are three river flow stations with highly correlated records, and *t* is time in days. The β coefficients were used to estimate missing observations in the station *y*. Correlated stations, correlation coefficients, and estimates of filling records are summarized in Table S1 in the Supplementary material.

4. Methods

4.1 Trends in rainfall and observed river flows

Analyses were carried out on 1976 to 2008 daily and monthly estimates of precipitation, river flow, and ET for the seven different spatial units described in Table 1, with the exception of river flow at Jamanxim, Itaituba, and Foz do Juruena, due to the large fraction of data missing for these stations. The Sheffield et al. (2006) dataset was analyzed at daily time steps and model's spatial resolution. River flow time series were analyzed based on hydrological years, assumed to start on August 1st (matching the end of the dry season) of each calendar year. Data were decomposed into monthly flows as well as 1-day, 3-day, 30-day, and 90-day minimum/maximum flows. The Mann-Kendall trend test was used to detect monotonic trends in the data.

4.2 Model evaluation of the influence of climate on river flows

Numerical simulations were carried out in order to isolate the direct effects of human disturbance/deforestation from the prescribed historical climate. The analysis was comprised of two hindcast simulations with different land cover transition histories, but everything else

being equal. Both simulations were carried out with 0.5° by 0.5° (roughly 55 km by 55 km) grid cells driven by identical climate observations from 1970 to 2008 (first six years not included in data analysis to avoid simulations' initialization effects) from Sheffield et al. (2006). The first simulation, 1970LC, represented a historical potential vegetation scenario in which land cover was fixed at its 1970 levels when forest cover in the Tapajós was 88%. Thus, any trends detected in river flows from this simulation could be attributed to climate variability. A second simulation, ContLC, resembled contemporary land cover changes by applying grid cell-level annual rates of land cover transitions as derived from Hurtt et al. (2006) and Soares-Filho et al., (2006) for the period 1970-2008. Since the purpose of this scenario is to replicate historical conditions, simulated flows and their trends were compared to river gauge observations for calibration and validation purposes (Figures S1 and S2, Table S4). A detail description of the calibration/validation is presented in Pereira et al. (2017) and summarized in Table 3 of this paper. Overall, all three coefficients of model fitness indicate an appropriate performance in the lower tributaries, but a tendency for Nash-Sutcliffe and Pearson's R coefficients to decrease in the headwaters was noticed. The simulated vs. observed volumetric ratio, however, was maintained near optimal values for most stations.

4.3 Model evaluation of the influence of deforestation on river flows

The basin studied experienced steady deforestation from the early 1980s to the late 2000s, from over 403,000 km^2 or 86% of the total basin area covered with forest in 1976, to less than 340,000 km^2 or 70% of the basin by 2008 (Figure 2). Overall, the sub-basins that experienced the greatest loss of forest, both in absolute and relative terms, were the lower Juruena and lower Teles Pires, where over 69,000 km^2 or 34% of the forest was cleared in the period 1976-2008 (Figure 2). While smaller in absolute terms (13,387 km^2), the upper Teles Pires experienced the largest relative deforestation rate among sub-basins (44%). Most of the deforested area in the Teles Pires and Juruena sub-basins has turned into pasture and soybean

cropland. In contrast, the lower and upper Tapajós sub-basins experienced a small gain in forest cover in both land cover datasets studied. Forest cover in the headwaters in the upper Juruena and Jamanxim sub-basin experienced mild changes, declining from 84 to 76% and from 93 to 89%, respectively.

Flow data for both scenarios, ContLC and 1970LC, were decomposed and analyzed in a similar fashion as described for the river gauge records in section 4.2. Once hydrological indicators were estimated, the difference in results between ContLC and 1970LC was estimated to infer the direct effects of deforestation on basin's hydrology. Total changes between the two simulations were also determined based on the non-parametric Kruskal-Wallis test for differences in variance. Differences between the simulations were also assessed via flow duration curves representing changes to daily river flow probability distributions. Changes in ET were assessed as one variable without making a distinction between its specific components (soil/leaf evaporation and transpiration) in the analysis. As previous modeling results of the effects on extreme deforestation on the regional Amazon hydrology show (Swann et al., 2015), net changes in total latent heat are primarily caused by changes in transpiration, while ground evaporation remains largely unaffected.

5. Results

5.1 Trends in rainfall and observed river flows

The trend analysis of monthly rainfall throughout the basin indicates little changes in total annual amounts, but shifts in seasonality were noticed. There are no clear trends in total annual rainfall in the Tapajós or any of its sub-basins during the period 1976-2008 (Figure 3; Table S2). However, time series of monthly rainfall indicate a contrast in spatial patterns across the basin, with significant shifts in the seasonal timing of rainfall in the headwaters and middle sub-basins and little change in the lower sub-basins (Figure 3). At the scale of the

Tapajós basin (Figure 3a), significant reductions in rainfall have occurred in the transition periods before and after the dry season, primarily in the months of May, September and December, and a significant positive trend in rainfall in January (wet season) rainfall. These trends were also evident at finer scales through the sub-basins, with rainfall decreases during the transitional months being particularly strong in the upper Juruena, lower Juruena, and upper Teles Pires (Figure 3e, f, and g, respectively). Overall, these shifts in rainfall monthly patterns are indicative of a concentration of rainfall in the late three months (January-March) of the wet season throughout the basin. The lower and upper Tapajós sub-basins showed a decrease in rainfall during the peak of the wet season (Figure 3c-d), although such changes were not statistically significant.

The trend analysis of river flows from 1976 to 2008 revealed a general tendency towards decreased flows during the dry season and transitional months (Figure 4). At the second furthest downstream station (Jatoba in the upper Tapajós), flows during the dry season months of July, August, and November, as well as early wet season (February) have decreased significantly, but not sufficient to significantly affect mean annual flows (Figure 4a; Table S3). At Tres Marias in the lower Teles Pires, significant negative trends were found through the six months of the dry season (June-November; Figure 4b). Trends at the furthest upstream gauges are remarkably different from each other, with significant negative trends in 11 months of the year (except for the wet month of February) at Fontanilhas in the upper Juruena (Figure 4c). In contrast, at Cachoeirão in the upper Teles Pires the only significant trend was an increase in flow during March, the peak of the wet season (Figure 4d). The significant negative trends estimated during the dry season and early rainy season months (July through November) resulted in significant negative trends in the 6-month moving average and 90-day minimum flows in all stations with the exception of Cachoeirão (Table

S3). Such negative trends were also sufficient to cause significant changes to mean annual flows at Tres Marias and Fontanhilas (Table S3).

5.2 Model evaluation of the influence of climate on river flows

The effects of changes in climate forcing were evaluated with a simulation of historical climate (1976-2008) with a static land cover state (no transitions) as in 1970. The results of this simulation indicate that some of the seasonal trends observed in river gauges are explained by trends in rainfall seasonality; in particular, flows during the transitional period from the end of the dry season to the start of the wet season. This seasonal difference is most clearly seen in the trends of simulated dry season flows, consistent with trends in the observed flow record (Table S3 and S4). In the 1970LC simulation that incorporates the effects of changes in climate forcing –but not land-use– 90-day minimum flow trends show a clear negative trend at Itaituba, the furthest downstream station (Figure 5a), and at Tres Marias in the lower Teles Pires in the middle of the basin (Figure 5d). These results deviate substantially from the ContLC simulation trend, incorporating both climate and deforestation effects, which show no clear trends in 90-day minimum flows through the time. Interestingly, 90-day minimum flows at Fontanilhas in the upper Juruena (Figure 5e) show a significant negative trend in flow in both the 1970LC and ContLC simulations. This consistency arises because of the minimal land cover change that occurred in this sub-basin in recent decades as observed in the Hurtt et al (2006) dataset (Figure 2).

5.3 Model evaluation of the influence of deforestation on river flows

By comparing the difference between the 1970LC (climate effects) and ContLC (climate and deforestation effects) simulations, we were able to evaluate the effect that deforestation has had on the magnitude of river flows. This difference reveals that the effect of deforestation appears to be clearest during the dry season months of July, August and September (Table 4). These flows correspond primarily to the 30-day and 90-day minimum

flow period, indicators which were found to be significantly different between the 1970LC and ContLC simulations for most locations (with the exception of Fontanilhas in the Upper Juruena; Figure 6e) according to the Kruskal-Wallis test (Table 4). This corresponds to the period of high exceedance probability, when the magnitude of water flows is low (Figure 6). Changes to low flows appear to be most evident in the middle sub-basins (Figure 6b, c, and d), which account for most of the contributing drainage areas where deforestation has historically occurred.

Differences in the time series of the 1970LC and ContLC simulations indicate that changes in flow (maximum of +4 mm month per month) were inversely proportional to trends in ET, though the magnitude of ET changes were always larger, presumably as a response to storage in the soil column. With exception of the upper Juruena, in which relative flow changes remained close to 1% as a result of limited land cover change (Figure 7e), results for all other subbasins showed that 3-4% monthly increase from the flow in the mid 1970s was triggered primarily once the deforested area reached approximately 20% of the drainage area (Figure 7). Alterations quantified in the furthest downstream gauges (Itaituba and Jatoba, Figure 7a and b), show that this breakpoint occurred during the early 1990s. These gauges at the lower end of our study basin, however, do not represent fully the spatial variability that occurred within the different sub-basins. For instance, in the lower and upper Teles Pires sub-basins (Figure 7d and f) the deforestation breakpoint of 20% was reached in the early 1980s, and as a result, percent change in flow relative to 1976 have increase steadily by 10-11%

6. Discussion

The results presented in this paper highlight the role that climate and land cover change have had on decadal trends and seasonal variability in water flows across a large tropical river basin. With regard to trends in rainfall, we found no significant changes in annual total rainfall, a result consistent with an earlier analysis of observations in the nearby Tocantins River (Costa et al., 2003). We did find, however, significant trends in rainfall seasonality over our study region, with decreases in monthly rainfall in the transitional months in the early and late dry season, and increases in rainfall during the month of January near the peak of the wet season (Figure 3). These shifts in seasonality accord with those reported through the Amazon and other tropical regions (Espinoza Villar et al., 2009b; Feng et al., 2013). Such trends are expected to have conflicting effects with deforestation by decreasing runoff during the transitional months. Indeed, trends in river flows were more evident in the headwaters and middle sub-basins, whereas the effects of the multiple drivers might have been offset in the downstream stations, as also pointed out by Moura (2015).

With regard to the effects of deforestation, the findings from the hindcast simulations presented in this paper are generally consistent with prior analyses of direct effects on flows in tropical rivers, showing that deforestation decreases ET and consequently increases river flow (Bruijnzeel, 2004; Wohl et al., 2012), process which has been demonstrated through field experiments (Brown et al., 2005), long term trend analyses (Coe et al., 2011; Costa et al., 2003) and modeling studies (Coe et al., 2009; Panday et al., 2015). In addition to this accepted general process, the results from this paper provide several insights regarding the temporally and spatially complex responses of river flows to deforestation.

First, we showed that deforestation effects have a greater influence on flows during the dry season than during the wet season (Table 4), finding also supported by a number of previous studies (e.g., Brown et al., 2005; Bruijnzeel, 2004; Ogden et al., 2013). Second, our

analysis showed that large river basins can have prolonged buffered capacity to withstand a certain level of deforestation, but effects on river flow become evident once deforestation levels reach a threshold (Figure 7). In the case of the Tapajós basin as a whole, we found that deforestation impacts on river flows started once the deforested area reached approximately 20% of the basin, which is in line with results from a modeling study in the neighboring Xingu basin (Panday et al., 2015).

Third, the results from this study highlight the spatial variability of deforestation effects along a river network, and how the significance of alterations can change as a function of rainfall patterns, as well as basin dimensions and spatial configuration (Figures 4 and 5). Large river basins covered by tropical rainforests are rather isolated, and often only monitored and studied based on a single or a few river gauges. As we showed in this paper, however, the effects of deforestation can be overlooked at locations of large flow accumulation, and instead, greatest effects were simulated in the middle of the basin directly at the outlets into which much of the deforested land drains. In general, responses of river flows to deforestation should be studied in terms of the spatial-temporal variation in hydroclimatology, topography, and land-cover in order to avoid the potentially misleading conclusions that can arise from basin-wide assessments.

Fourth, the results from this study show how the conflicting effects of land-use change and climate forcing can account for the dismissal of the expected positive effect of deforestation on river flows. Although we show significant differences in dry season flows between our simulations (Table 4), such differences –driven by deforestation– were not large enough to be evident in river gauge records. The analysis of trends from the 1970LC (climate effects only, no deforestation) scenario, implies that multi-decadal rainfall variability is likely to be at least partially responsible for masking the deforestation effects from most of the observed river flow records. A similar argument was made regarding attribution of river flow

change in the adjacent Xingu River. Panday et al. (2015) used the model IBIS to indicate that a net decrease of 48 mm yr^{-1} in annual discharge from the 1970s to 2000s in the Xingu was the net result of a +34 mm yr^{-1} increase (+6%) caused by deforestation, in combination with a larger discharge reduction in flow of 82 mm yr^{-1} (-14%), caused by climate variability. Overall, simulations from both Panday et al. (2015) and this study highlight the complexity behind hydrological alterations in these large tropical basins and the important role that numerical models can have in attributing cause-and-effect to climate, deforestation, and other environmental factors driving alterations in river flow.

The methodology used here with ED2, a land-surface model incorporating dynamic land-use change and coupled with a flow routing scheme (+R), represents a significant advancement in the study of deforestation on large river basins, which has been traditionally addressed with hydrological models that seldom consider the effects of fine-scale vegetation patterns and annual land-use dynamics on water fluxes. Using modeling scenarios with static/dynamic land-use change, it was possible to isolate the direct impacts of deforestation on the magnitude and seasonality of water flows, and demonstrated that such effects vary temporally and spatially according to the contemporary land cover transitions that occurred throughout the basin.

Three caveats apply to the findings of this study. First, the spatial resolution of the climate forcing dataset used in this study may be coarser than what is commonly used for meso-scale basin hydrological studies. Future efforts to incorporate finer scale input data may decrease the uncertainty related to climate forcing. Second, while our analysis incorporated the direct effects of rainfall variability and land-use change, it excluded the indirect effects of how land-use change can cause a feedback an affect regional patterns of rainfall, which previous theoretical and/or modeling studies indicated that may lead to decreases in rainfall (Coe et al., 2009; Davidson et al., 2012; Makarieva and Gorshkov, 2006; Sampaio et al.,

2007; Stickler et al., 2013; Swann et al., 2015; Wang and Eltahir, 2000). This feedback, however, may only be relevant at very large scales and there is no observed evidence of its effects on hydrology in the Amazon or elsewhere in the tropics (Costa et al., 2010, 2003; Wilk et al., 2001). The third caveat of this study is related to the potential long-term effects of deforestation on soil hydraulic characteristics, groundwater recharge, and baseflow. Bruijnzeel (2004) postulated that *"…in the longer term rainfall infiltration is often reduced to the extent that insufficient rainy season replenishment of groundwater reserves results in strong declines in dry season flows"*. At comparable large scales, changes in hydrological processes suggesting decreased soil hydraulic conductivity were reported in the Australian dry tropics (Peña-Arancibia et al., 2012). There is also evidence of decreased soil hydraulic conductivity following land-use intensification in the headwaters of the adjacent Xingu river (Scheffler et al., 2011), suggesting that this could also have occurred in the headwaters of our study region. The complex, fine-scale, and dynamic interactions between land cover, soil hydraulic properties and baseflow are critical limitations that other land-surface models also have in representing tropical hydrology (Zulkafli et al., 2013), and this is certainly a key aspect that requires further research in future studies.

7. Conclusion

This paper analyzed recent historical trends in river flows in a large tropical river basin and the contribution that climate variability and deforestation have had during the hydrological transition faced in recent decades. This was accomplished by analyzing trends in rainfall, land cover, and river flows throughout the basin, and by combining them with hindcast simulations that decoupled deforestation effects from the observed climate forcing. Deforestation rates were steady from the late 1970s until the early 2000s, but then increased drastically, in particular in the middle sub-basins. During this same period, we found no

trends in annual rainfall, although shifts in seasonality did in fact occur, mainly as a concentration of rainfall during the peak of the wet season. Numerical simulations with ED2+R revealed that deforestation has gradually decreased ET, in particular in the middle sub-basins, which caused measurable increases in dry season flows once total forest cover was reduced below 80%. As we showed, however, changes in rainfall seasonality affected flows during the dry season in opposite direction and greater magnitude, masking deforestation effects, and finally resulting in the net negative trends in 90-day minimum flows found in the observed flow records.

The Tapajós basin is going through a critical phase of transition that mirrors what is occurring in the greater Amazon and other tropical rainforests around the world. Climate variability and environmental degradation are the primary biophysical drivers of change, and major tradeoffs are expected with regards to biodiversity and infrastructure development. Agriculture and hydropower, in particular, are socio-economic sectors that are playing an increasingly important role in the economy and water cycle of the Amazon and other large tropical rivers, and consequently, it is fundamental to continue to investigate how water resources have been affected by regional and global change in the past and how they will continue to interplay with these drivers of change in the future.

Acknowledgements

The authors would like to dedicate this study to the late Professor John Briscoe (1948 - 2014), who envisioned and co-led the Amazon Initiative of Harvard's Sustainability Science Program. This work was conducted while M.E. Arias, E. Lee, F. Farinosi, and F. Pereira were Giorgio Ruffolo Fellows in the Sustainability Science Program at Harvard University. Support from Italy's Ministry for Environment, Land and Sea is gratefully acknowledged. F. Farinosi was also funded through a doctoral scholarship by Ca' Foscari University of Venice.

We would like to thank Angela Livino and two anonymous reviewers for their valuable comments on this manuscript.

References

Albani, M., Medvigy, D., Hurtt, G.C., Moorcroft, P.R., 2006. The contributions of land- use change, CO2 fertilization, and climate variability to the Eastern US carbon sink. Global Change Biology 12, 2370–2390.

ANA, 2011. Water Resources Strategic Plan of the right margin of the Amazon River.

Beck, H.E., Bruijnzeel, L.A., Van Dijk, A., McVicar, T.R., Scatena, F.N., Schellekens, J., 2013. The impact of forest regeneration on streamflow in 12 mesoscale humid tropical catchments. Hydrology and Earth System Sciences 17, 2613–2635.

Bonell, M., Bruijnzeel, L.A., 2005. Forests, water and people in the humid tropics: past, present and future hydrological research for integrated land and water management. Cambridge University Press.

Brown, A.E., Zhang, L., McMahon, T.A., Western, A.W., Vertessy, R.A., 2005. A review of paired catchment studies for determining changes in water yield resulting from alterations in vegetation. Journal of Hydrology 310, 28–61. https://doi.org/10.1016/j.jhydrol.2004.12.010

Bruijnzeel, L.A., 2004. Hydrological functions of tropical forests: not seeing the soil for the trees? Agriculture, Ecosystems & Environment 104, 185–228.

Butt, N., de Oliveira, P.A., Costa, M.H., 2011. Evidence that deforestation affects the onset of the rainy season in Rondonia, Brazil. Journal of Geophysical Research 116. https://doi.org/10.1029/2010JD015174

Coe, M.T., Costa, M.H., Soares-Filho, B.S., 2009. The influence of historical and potential future deforestation on the stream flow of the Amazon River – Land surface processes and atmospheric feedbacks. Journal of Hydrology 369, 165–174. https://doi.org/10.1016/j.jhydrol.2009.02.043

Coe, M.T., Latrubesse, E.M., Ferreira, M.E., Amsler, M.L., 2011. The effects of deforestation and climate variability on the streamflow of the Araguaia River, Brazil. Biogeochemistry 105, 119–131. https://doi.org/10.1007/s10533-011-9582-2

Coe, M.T., Marthews, T.R., Costa, M.H., Galbraith, D.R., Greenglass, N.L., Imbuzeiro, H.M.A., Levine, N.M., Malhi, Y., Moorcroft, P.R., Muza, M.N., Powell, T.L., Saleska, S.R., Solorzano, L.A., Wang, J., 2013. Deforestation and climate feedbacks threaten the ecological integrity of south–southeastern Amazonia. Philosophical Transactions of the Royal Society B: Biological Sciences 368. https://doi.org/10.1098/rstb.2012.0155

Collischonn, W., Allasia, D., Da Silva, B.C., Tucci, C.E.M., 2007. The MGB-IPH model for large-scale rainfall—runoff modelling. Hydrological Sciences Journal 52, 878–895. https://doi.org/10.1623/hysj.52.5.878

Costa, M.H., Biajoli, M.C., Sanches, L., Malhado, A., Hutyra, L.R., Da Rocha, H.R., Aguiar, R.G., de Araújo, A.C., 2010. Atmospheric versus vegetation controls of Amazonian tropical rain forest evapotranspiration: are the wet and seasonally dry rain forests any different? Journal of Geophysical Research: Biogeosciences 115.

Costa, M.H., Botta, A., Cardille, J.A., 2003. Effects of large-scale changes in land cover on the discharge of the Tocantins River, Southeastern Amazonia. Journal of Hydrology 283, 206–217.

Costa, M.H., Foley, J.A., 1997. Water balance of the Amazon Basin: Dependence on vegetation cover and canopy conductance. J. Geophys. Res. 102, 23973–23989. https://doi.org/10.1029/97JD01865

Davidson, E.A., de Araujo, A.C., Artaxo, P., Balch, J.K., Brown, I.F., C. Bustamante, M.M., Coe, M.T., DeFries, R.S., Keller, M., Longo, M., Munger, J.W., Schroeder, W., Soares-Filho, B.S., Souza, C.M., Wofsy, S.C., 2012. The Amazon basin in transition. Nature 481, 321–328. https://doi.org/10.1038/nature10717

DiMiceli, C.M., Carroll, M.L., Sohlberg, R.A., Huang, C., Hansen, M.C., Townshend, J.R.G., 2011. Annual global automated MODIS vegetation continuous fields (MOD44B) at 250 m spatial resolution for data years beginning day 65, 2000-2010, collection 5 percent tree cover. USA: University of Maryland, College Park, MD.

Espinoza Villar, J.C., Guyot, J.L., Ronchail, J., Cochonneau, G., Filizola, N., Fraizy, P., Labat, D., de Oliveira, E., Ordoñez, J.J., Vauchel, P., 2009a. Contrasting regional discharge evolutions in the Amazon basin (1974–2004). Journal of Hydrology 375, 297–311. https://doi.org/10.1016/j.jhydrol.2009.03.004

Espinoza Villar, J.C., Ronchail, J., Guyot, J.L., Cochonneau, G., Naziano, F., Lavado, W., De Oliveira, E., Pombosa, R., Vauchel, P., 2009b. Spatio-temporal rainfall variability in the Amazon basin countries (Brazil, Peru, Bolivia, Colombia, and Ecuador). Int. J. Climatol. 29, 1574–1594. https://doi.org/10.1002/joc.1791

Farquhar, G. v, von Caemmerer, S. von, Berry, J.A., 1980. A biochemical model of photosynthetic CO2 assimilation in leaves of C3 species. Planta 149, 78–90.

Feng, X., Porporato, A., Rodriguez-Iturbe, I., 2013. Changes in rainfall seasonality in the tropics. Nature Clim. Change 3, 811–815.

Getirana, A.C.V., Dutra, E., Guimberteau, M., Kam, J., Li, H.-Y., Decharme, B., Zhang, Z., Ducharne, A., Boone, A., Balsamo, G., Rodell, M., Toure, A.M., Xue, Y., Peters-Lidard, C.D., Kumar, S.V., Arsenault, K., Drapeau, G., Ruby Leung, L., Ronchail, J., Sheffield, J., 2014. Water Balance in the Amazon Basin from a Land Surface Model Ensemble. Journal of Hydrometeorology 15, 2586–2614. https://doi.org/10.1175/JHM-D-14-0068.1

Gloor, M., Brienen, R.J.W., Galbraith, D., Feldpausch, T.R., Schöngart, J., Guyot, J.-L., Espinoza, J.C., Lloyd, J., Phillips, O.L., 2013. Intensification of the Amazon hydrological cycle over the last two decades. Geophys. Res. Lett. 40, 1729–1733. https://doi.org/10.1002/grl.50377

Hayhoe, S.J., Neill, C., Porder, S., McHorney, R., Lefebvre, P., Coe, M.T., Elsenbeer, H., Krusche, A.V., 2011. Conversion to soy on the Amazonian agricultural frontier increases streamflow without affecting stormflow dynamics. Global Change Biology 17, 1821–1833. https://doi.org/10.1111/j.1365-2486.2011.02392.x

Hurtt, G.C., Frolking, S., Fearon, M.G., Moore, B., Shevliakova, E., Malyshev, S., Pacala, S.W., Houghton, R.A., 2006. The underpinnings of land-use history: three centuries of global gridded land-use transitions, wood-harvest activity, and resulting secondary lands. Global Change Biology 12, 1208–1229. https://doi.org/10.1111/j.1365-2486.2006.01150.x

Kim, Y., Knox, R.G., Longo, M., Medvigy, D., Hutyra, L.R., Pyle, E.H., Wofsy, S.C., Bras, R.L., Moorcroft, P.R., 2012. Seasonal carbon dynamics and water fluxes in an Amazon rainforest. Glob Change Biol 18, 1322–1334. https://doi.org/10.1111/j.1365-2486.2011.02629.x

Knox, R., Bisht, G., Wang, J., Bras, R., 2010. Precipitation Variability over the Forest-to-Nonforest Transition in Southwestern Amazonia. J. Climate 24, 2368–2377. https://doi.org/10.1175/2010JCLI3815.1

Knox, R.G., Longo, M., Swann, A.L., Zhang, K., Levine, N.M., Moorcroft, P.R., Bras, R.L., 2015. Hydrometeorological effects of historical land-conversion in an ecosystem-atmosphere model of Northern South America. Hydrology and Earth System Sciences 19, 241–273.

Leite, C.C., Costa, M.H., de Lima, C.A., Ribeiro, C.A.A.S., Sediyama, G.C., 2010. Historical reconstruction of land use in the Brazilian Amazon (1940–1995). Journal of Land Use Science 6, 33–52. https://doi.org/10.1080/1747423X.2010.501157

Leuning, R., 1995. A critical appraisal of a combined stomatal- photosynthesis model for C3 plants. Plant, Cell & Environment 18, 339–355.

Levine, N.M., Zhang, K., Longo, M., Baccini, A., Phillips, O.L., Lewis, S.L., Alvarez-Dávila, E., Segalin de Andrade, A.C., Brienen, R.J.W., Erwin, T.L., Feldpausch, T.R., Monteagudo Mendoza, A.L., Nuñez Vargas, P., Prieto, A., Silva-Espejo, J.E., Malhi, Y., Moorcroft, P.R., 2016. Ecosystem heterogeneity determines the ecological resilience of the Amazon to climate change. Proceedings of the National Academy of Sciences 113, 793–797. https://doi.org/10.1073/pnas.1511344112

Lewis, S.L., Edwards, D.P., Galbraith, D., 2015. Increasing human dominance of tropical forests. Science 349, 827–832. https://doi.org/10.1126/science.aaa9932

Longo, M., 2014. Amazon Forest Response to Changes in Rainfall Regime: Results from an Individual-Based Dynamic Vegetation Model (PhD thesis). Harvard University, Cambridge, MA, USA.

Makarieva, A.M., Gorshkov, V.G., 2006. Biotic pump of atmospheric moisture as driver of the hydrological cycle on land. Hydrology and Earth System Sciences Discussions 3, 2621–2673.

Malhi, Y., Roberts, J.T., Betts, R.A., Killeen, T.J., Li, W., Nobre, C.A., 2008. Climate Change, Deforestation, and the Fate of the Amazon. Science 319, 169–172. https://doi.org/10.1126/science.1146961

Marengo, J.A., 2004. Interdecadal variability and trends of rainfall across the Amazon basin. Theor Appl Climatol 78, 79–96. https://doi.org/10.1007/s00704-004-0045-8

Medvigy, D., Wofsy, S.C., Munger, J.W., Hollinger, D.Y., Moorcroft, P.R., 2009. Mechanistic scaling of ecosystem function and dynamics in space and time: Ecosystem Demography model version 2. J. Geophys. Res. 114, G01002. https://doi.org/10.1029/2008JG000812

Moorcroft, P.R., Hurtt, G.C., Pacala, S.W., 2001. A method for scaling vegetation dynamics: The Ecosystem Demography Model (ED). Ecological Monographs 71, 557–586. https://doi.org/10.1890/0012-9615(2001)071[0557:AMFSVD]2.0.CO;2

Morton, D.C., DeFries, R.S., Shimabukuro, Y.E., Anderson, L.O., Arai, E., del Bon Espirito-Santo, F., Freitas, R., Morisette, J., 2006. Cropland expansion changes deforestation dynamics in the southern Brazilian Amazon. Proceedings of the National Academy of Sciences 103, 14637–14641. https://doi.org/10.1073/pnas.0606377103

Moura, L.Z., 2015. Evaluation of monotonic trends for streamflow in austral Amazon, Brazil: a case study for the Xingu and Tapajós rivers. Proceedings of the International Association of Hydrological Sciences 371, 125.

Neill, C., Coe, M.T., Riskin, S.H., Krusche, A.V., Elsenbeer, H., Macedo, M.N., McHorney, R., Lefebvre, P., Davidson, E.A., Scheffler, R., Figueira, A.M. e S., Porder, S., Deegan, L.A., 2013. Watershed responses to Amazon soya bean cropland expansion and intensification. Philosophical Transactions of the Royal Society of London B: Biological Sciences 368. https://doi.org/10.1098/rstb.2012.0425

Ogden, F.L., Crouch, T.D., Stallard, R.F., Hall, J.S., 2013. Effect of land cover and use on dry season river runoff, runoff efficiency, and peak storm runoff in the seasonal tropics of Central Panama. Water Resources Research 49, 8443–8462.

Panday, P.K., Coe, M.T., Macedo, M.N., Lefebvre, P., Castanho, A. de A., 2015. Deforestation offsets water balance changes due to climate variability in the Xingu River in eastern Amazonia. Journal of Hydrology 523, 822–829. https://doi.org/10.1016/j.jhydrol.2015.02.018

Peña-Arancibia, J.L., van Dijk, A.I., Guerschman, J.P., Mulligan, M., Bruijnzeel, L.A.S., McVicar, T.R., 2012. Detecting changes in streamflow after partial woodland clearing in two large catchments in the seasonal tropics. Journal of Hydrology 416, 60–71.

Pereira, F.F., Farinosi, F., Arias, M.E., Lee, E., Briscoe, J., Moorcroft, P.R., 2017. Technical note: A hydrological routing scheme for the Ecosystem Demography model (ED2+R) tested in the Tapajós River basin in the Brazilian Amazon. Hydrol. Earth Syst. Sci. 21, 4629. http://dx.doi.org/10.5194/hess-21-4629-2017

Powell, T.L., 2015. Determining drought sensitivity of the Amazon forest: does plant hydraulics matter? (Doctoral Dissertation). Harvard University, Cambridge, MA, USA.

Rodriguez, D.A., Tomasella, J., Linhares, C., 2010. Is the forest conversion to pasture affecting the hydrological response of Amazonian catchments? Signals in the Ji-Paraná Basin. Hydrological Processes 24, 1254–1269.

Sampaio, G., Nobre, C., Costa, M.H., Satyamurty, P., Soares- Filho, B.S., Cardoso, M., 2007. Regional climate change over eastern Amazonia caused by pasture and soybean cropland expansion. Geophysical Research Letters 34.

Scheffler, R., Neill, C., Krusche, A.V., Elsenbeer, H., 2011. Soil hydraulic response to land-use change associated with the recent soybean expansion at the Amazon agricultural frontier. Agriculture, Ecosystems & Environment 144, 281–289. https://doi.org/10.1016/j.agee.2011.08.016

Sheffield, J., Goteti, G., Wood, E.F., 2006. Development of a 50-year high-resolution global dataset of meteorological forcings for land surface modeling. Journal of Climate 19, 3088–3111.

Soares-Filho, B.S., Nepstad, D.C., Curran, L.M., Cerqueira, G.C., Garcia, R.A., Ramos, C.A., Voll, E., McDonald, A., Lefebvre, P., Schlesinger, P., 2006. Modelling conservation in the Amazon basin. Nature 440, 520–523. https://doi.org/10.1038/nature04389

Spracklen, D.V., Arnold, S.R., Taylor, C.M., 2012. Observations of increased tropical rainfall preceded by air passage over forests. Nature 489, 282–285. https://doi.org/10.1038/nature11390

Stickler, C.M., Coe, M.T., Costa, M.H., Nepstad, D.C., McGrath, D.G., Dias, L.C.P., Rodrigues, H.O., Soares-Filho, B.S., 2013. Dependence of hydropower energy generation on forests in the Amazon Basin at local and regional scales. Proceedings of the National Academy of Sciences 110, 9601–9606. https://doi.org/10.1073/pnas.1215331110

Swann, A.L.S., Longo, M., Knox, R.G., Lee, E., Moorcroft, P.R., 2015. Future deforestation in the Amazon and consequences for South American climate. Agricultural and Forest Meteorology 214–215, 12–24. https://doi.org/10.1016/j.agrformet.2015.07.006

Van der Ent, R.J., Savenije, H.H., Schaefli, B., Steele- Dunne, S.C., 2010. Origin and fate of atmospheric moisture over continents. Water Resources Research 46.

Wang, G., Eltahir, E.A., 2000. Role of vegetation dynamics in enhancing the low- frequency variability of the Sahel rainfall. Water Resources Research 36, 1013–1021.

Wilk, J., Andersson, L., Plermkamon, V., 2001. Hydrological impacts of forest conversion to agriculture in a large river basin in northeast Thailand. Hydrological Processes 15, 2729–2748.

Wohl, E., Barros, A., Brunsell, N., Chappell, N.A., Coe, M., Giambelluca, T., Goldsmith, S., Harmon, R., Hendrickx, J.M.H., Juvik, J., McDonnell, J., Ogden, F., 2012. The

hydrology of the humid tropics. Nature Clim. Change 2, 655–662. https://doi.org/10.1038/nclimate1556

Wohlfahrt, G., Bianchi, K., Cernusca, A., 2006. Leaf and stem maximum water storage capacity of herbaceous plants in a mountain meadow. Journal of hydrology 319, 383–390.

WWF/TNC, 2013. Freshwater Ecoregions Of the World: Tapajos - Juruena [WWW Document]. URL http://www.feow.org/ecoregions/details/320 (accessed 8.5.15).

Yang, Y., Donohue, R.J., McVicar, T.R., Roderick, M.L., Beck, H.E., 2016. Long- term CO2 fertilization increases vegetation productivity and has little effect on hydrological partitioning in tropical rainforests. Journal of Geophysical Research: Biogeosciences 121, 2125–2140.

Zhang, K., Castanho, A.D. de A., Galbraith, D.R., Moghim, S., Levine, N., Bras, R.L., Coe, M., Costa, M.H., Malhi, Y., Longo, M., Knox, R.G., McKnight, S., Wang, J., Moorcroft, P.R., 2015. The Fate of Amazonian Ecosystems over the Coming Century Arising from Changes in Climate, Atmospheric CO2 and Land-use. Glob Change Biol 21, 2569–2587. https://doi.org/10.1111/gcb.12903

Zulkafli, Z., Buytaert, W., Onof, C., Lavado, W., Guyot, J.L., 2013. A critical assessment of the JULES land surface model hydrology for humid tropical environments. Hydrol. Earth Syst. Sci. 17, 1113–1132. https://doi.org/10.5194/hess-17-1113-2013

Table 1. Description of Tapajós sub-basins used in the study. Please see Table 2 for data sources.

Sub-basin	Sub-basin area, m^2	Cumulative contributing area, m^2	Main river gauge station	Mean annual rainfall (range), mm	Mean monthly river flow (range), m^3/s
Jamanxim	58,594	58,594	Jamanxim	2,191 (1,865-2,433	1,143 (137-4,405)
Upper Teles Pires	34,652	34,652	Cachoeirão	1,955 (1,274-2,592)	849 (307-2,287)
Upper Juruena	55,918	55,918	Fontanilhas	1,799 (1,307-2,196)	1,462 (1,057-2,180)
Lower Teles Pires	103,829	138,481	Tres Marias	2,253 (1,960-2,443)	3,741 (861-10,362)
Lower Juruena	135,391	191,309	Foz do Juruena	2,115 (1,656-2,574)	4,715 (1,766-11,348)
Upper Tapajós	57,767	352,905	Jatoba	2,266 (1,881-2,543)	10,791 (3,300-27,928)
Lower Tapajós	30,523	476,674	Itaituba	2014 (1,533-2,624)	11,881 (2,307-28,639)
Total domain (Tapajós Basin)	476,674	476,674	Itaituba	2,115 (1,867-2,366)	

Table 2. Summary of data used for this study.

Data type	Description	Resolution	Source
Climate	Global reanalysis of atmospheric temperature, specific humidity, downward shortwave/long-wave radiation, wind speed, air pressure, and precipitation	3-hourly (temporal); 1° (spatial)	Sheffield et al. (2006)
Soils	Soil type and texture fractions; water retention characteristics	1° (spatial)	Quesada et al. (2010) and Cosby et al. (1984).
Land-use history	Transitions among agriculture, primary and secondary vegetation	1° (spatial)	Hurtt et al. (2006), Soares-Filho et al. (2006)
River flow	All available records for 15 stations in 3 rivers	Daily	www2.snirh.gov.br; www.ore-hybam.org

Table 3. Summary of calibration and validation of ED2+R for the Tapajos using the dynamic land cover scenario (ContLC). Simulated vs observed volume ratio (V), Nash-Sutcliffe (NS), and Pearson's R optimal value is 1. Results presented for daily|monthly time series. Please see Pereira et al. (2017) for a detail description of the calibration/validation procedure.

Sub-basin	Calibration period (1976-1992)			Validation period (1993-2008)		
	NS	R	V	NS	R	V
Upper Juruena	0.45|0.46	0.68|0.69	0.98|0.98	0.29|0.32	0.54|0.57	1.01|1.01
Upper Teles Pires	0.37|0.43	0.64|0.68	1.01|0.99	0.28|0.34	0.63|0.67	1.03|1.04
Lower Juruena	0.65|0.69	0.82|0.85	0.94|0.96	0.63|0.67	0.81|0.84	1.08|1.09
Lower Teles Pires	0.70|0.74	0.85|0.88	1.02|1.01	0.67|0.70	0.85|0.88	1.17|1.16
Jamanxim	0.67|0.71	0.85|0.87	1.13|1.13	0.55|0.58	0.77|0.78	1.09|1.06
Upper Tapajós	0.77|0.80	0.88|0.90	0.99|1.01	0.75|0.79	0.88|0.90	1.08|1.08
Lower Tapajós	0.76|0.80	0.88|0.91	1.06|1.08	0.68|0.72	0.86|0.88	1.13|1.12

Table 4. Results of the non-parametric Kruskal-Wallis statistic test (X^2) for significant differences between flow indicators for the two computer simulations carried out. Statistically significant differences highlight the seasonal indicators that were affected by land cover change.

	Itaituba (Lower Tapajós)		Jatoba (Upper Tapajós)		Foz do Juruena (Lower Juruena)		Tres Marias (Lower Teles Pires)		Fontanilhas (Upper Juruena)		Cachoeirão (Upper Teles Pires)	
Indicator	X^2	p	X^2	p	X^2	P	X^2	p	X^2	p	X^2	p
August	16.43	***	19.42	***	15.36	***	25.12	***	1.17		2.96	*
September	18.41	***	20.09	***	13.51	***	23.46	***	0.80		4.92	**
October	3.41	*	3.51	*	2.67	*	6.58	***	1.06		0.82	
November	0.82		0.74		0.23		0.99		0.40		0.08	
December	0.88		0.90		0.36		1.58		0.26		0.05	
January	0.91		1.16		2.93	*	9.64	***	0.35		0.28	
February	1.17		1.04		3.15	*	5.63	**	0.26		1.19	
March	0.51		0.77		0.99		1.13		0.26		0.38	
April	0.63		0.81		0.99		2.06		0.41		0.36	
May	1.42		1.00		1.71		2.98	*	0.55		0.76	
June	2.14		3.06	*	6.26	***	10.91	***	0.69		0.62	
July	10.95	***	14.12	***	13.05	***	23.84	***	0.64		1.53	
1-day min	17.97	***	22.16	***	15.62	***	28.24	***	1.07		5.70	**
3-day min	18.74	***	22.46	***	15.71	***	28.13	***	1.15		5.51	**
7-day min	17.43	***	21.91	***	15.60	***	28.13	***	1.10		5.21	**
30-day min	15.55	***	20.61	***	16.01	***	27.85	***	1.08		4.16	**
90-day min	9.24	***	10.82	***	9.20	***	16.42	***	1.16		2.01	
1-day max	0.39		0.55		0.85		0.77		0.24		0.36	
3-day max	0.37		0.52		0.88		0.76		0.26		0.36	
7-day max	0.30		0.43		0.88		0.94		0.26		0.33	
30-day max	0.45		0.62		0.89		1.29		0.26		0.32	
90-day max	0.94		1.12		1.42		3.82	*	0.29		0.53	

Statistical significant levels: *: $p \leq 0.1$; ** $p \leq 0.05$; ***: $p \leq 0.01$

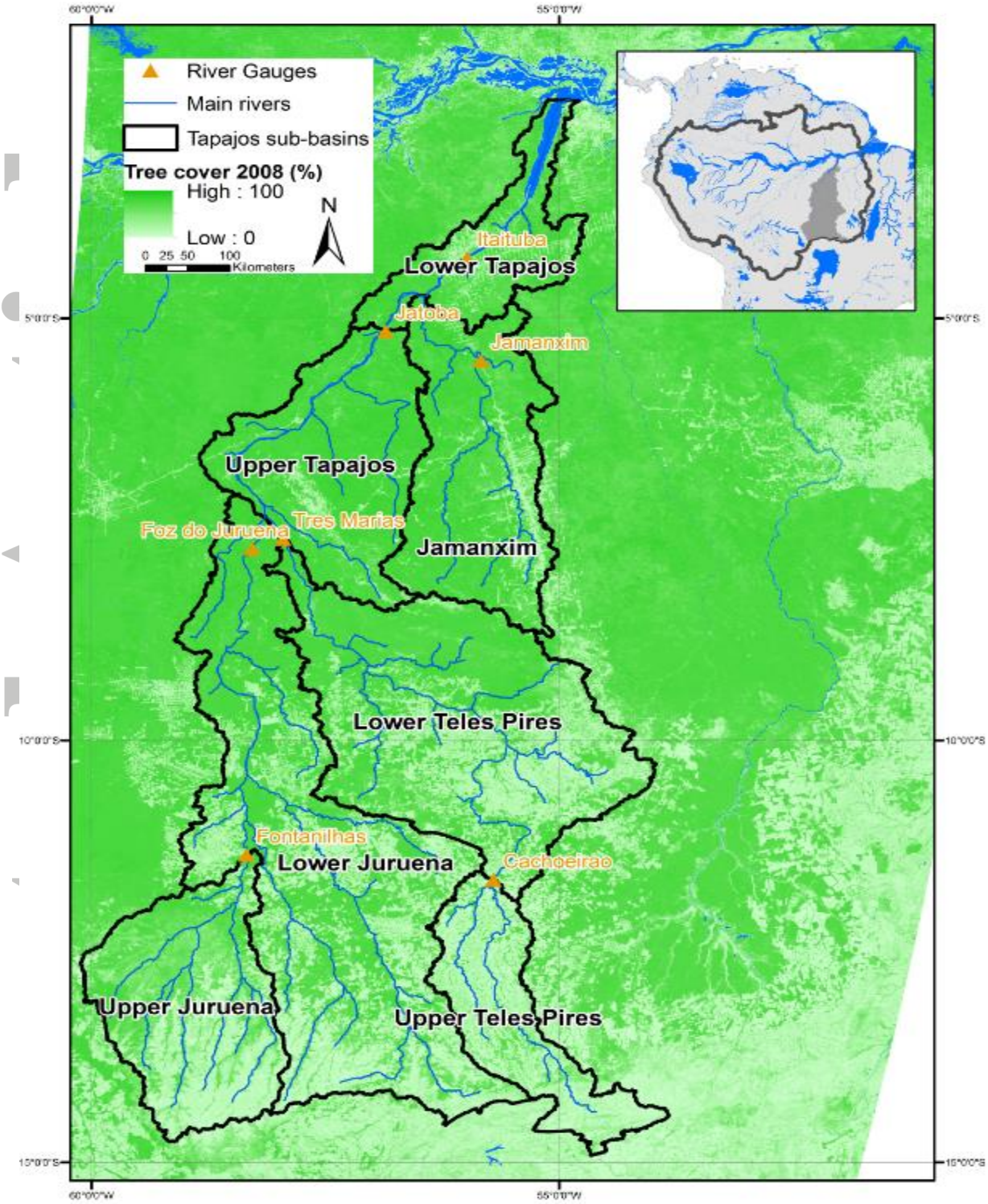

Figure 1. Map of the Tapajós river basin highlighting seven study sub-basins, and monitoring stations. The tree cover for 2008 (scaled in green) was derived from MODIS observations by DiMiceli et al. (2011).

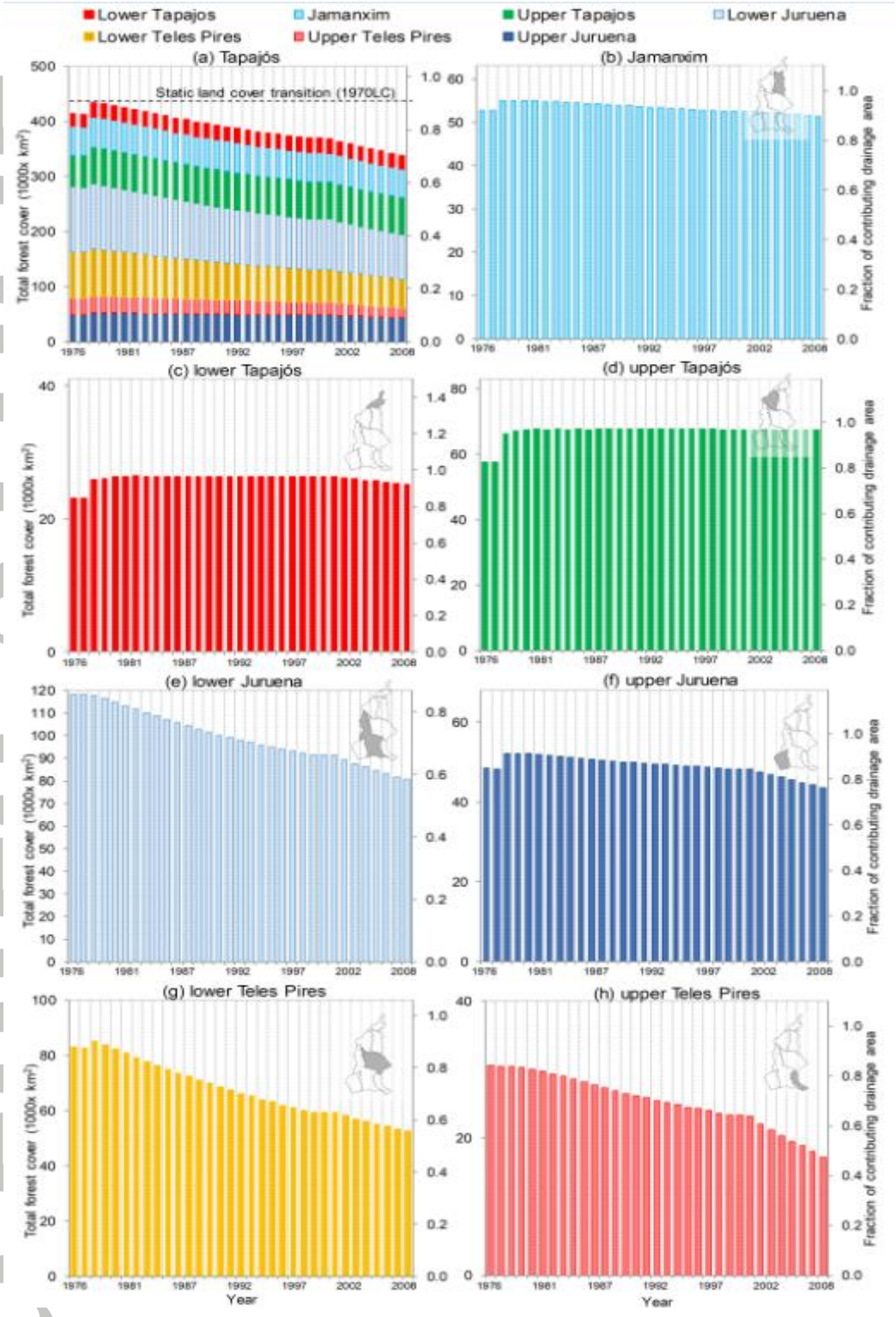

Figure 2. Summary of forest cover changes at the sub-basin scale. Data from Hurtt et al. (2006) up to 2000, and from Soares-Filho et al. (2006) for the remaining years. The dashed black line in frame (a) represents the LC1970 simulation with no land cover transitions since 1970.

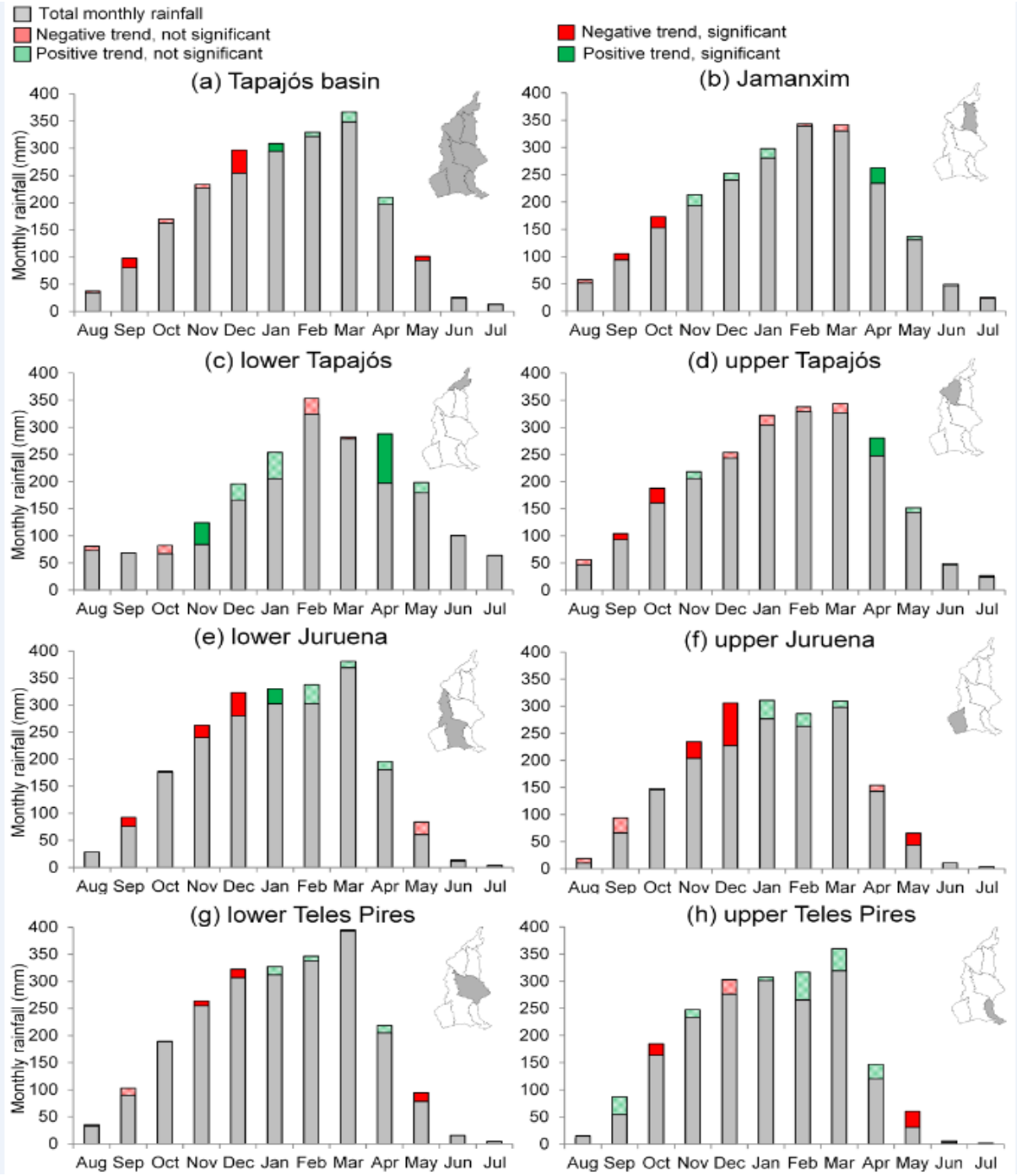

Figure 3. Monthly total rainfall in the Tapajos and sub-basins. Statistical significance of trends according to the Mann-Kendall test at the 0.9 confidence level. The height of the colored portion of bars represents the magnitude of change between the first (76-85) and last (99-08) decades in the analysis. Detail results of the statistical test for rainfall trends are presented in Table S2.

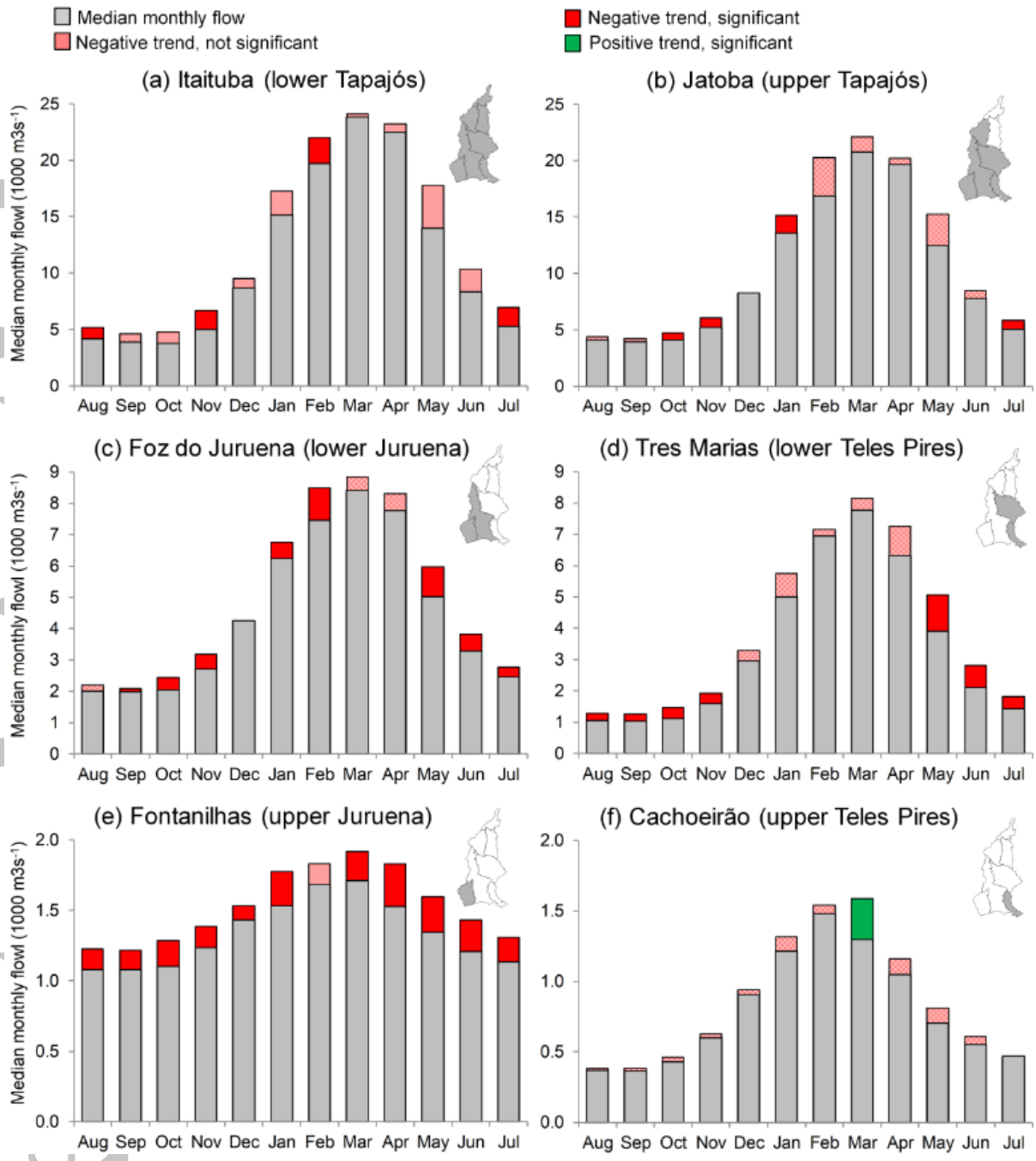

Figure 4. Observed monthly mean flows in selected Tapajós sub-basins during 1976-2008. The statistical significance of trends is according to the Mann-Kendall test at the 0.9 confidence level. Height of colored portion of bars represents the magnitude of change between the first (76-85) and last (99-08) decades in the analysis. Detail results of the statistical test for flow trends are presented in Table S3. Stations where a majority of records came from interpolated data were excluded.

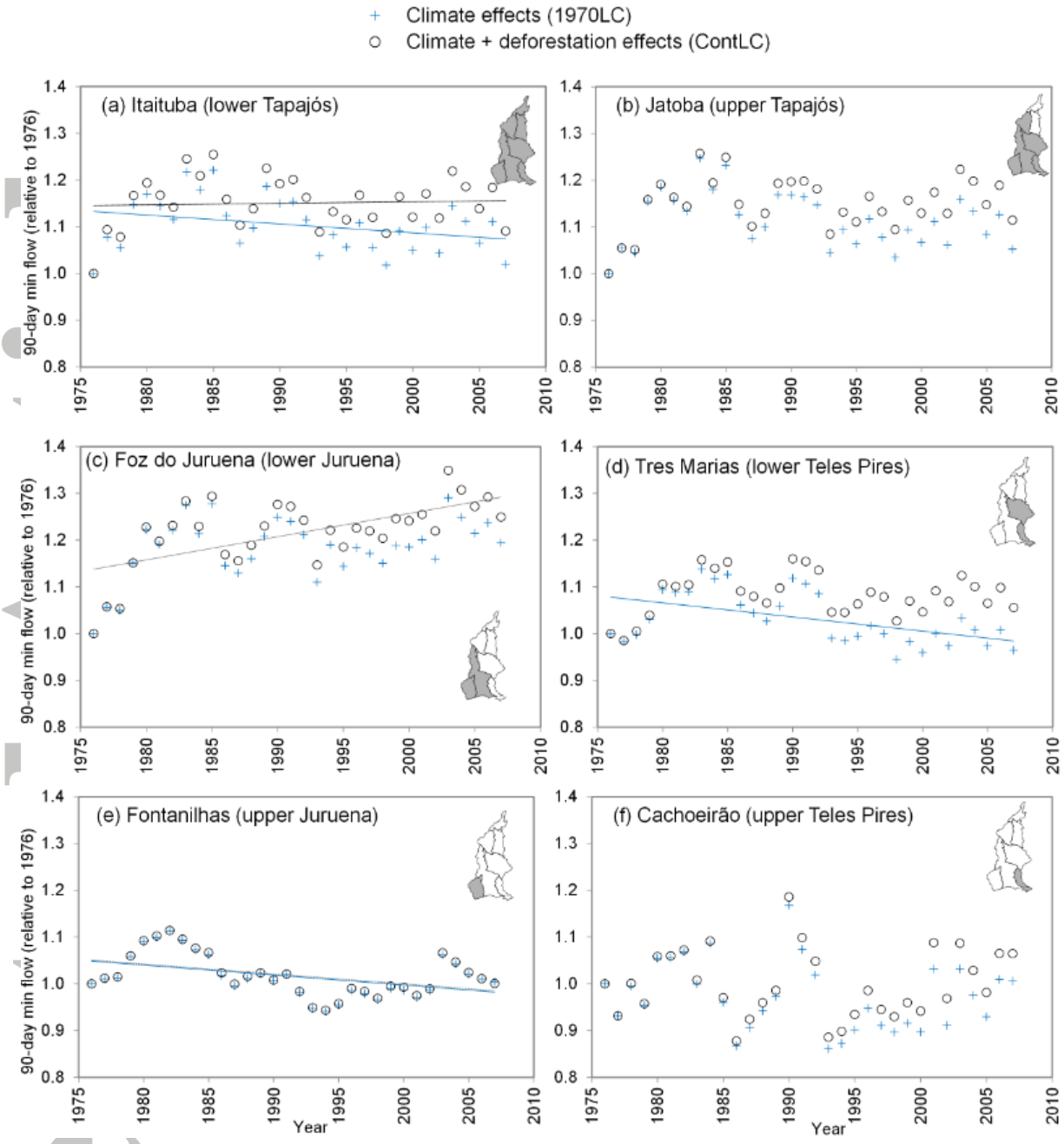

Figure 5. Time series of 90-day minimum flows (relative to the 90-day minimum flow in 1976) for the simulations of climate effects alone (1970LC) and climate with land cover transitions (ContLC). Regression lines represent significant trends ($p \leq 0.1$).

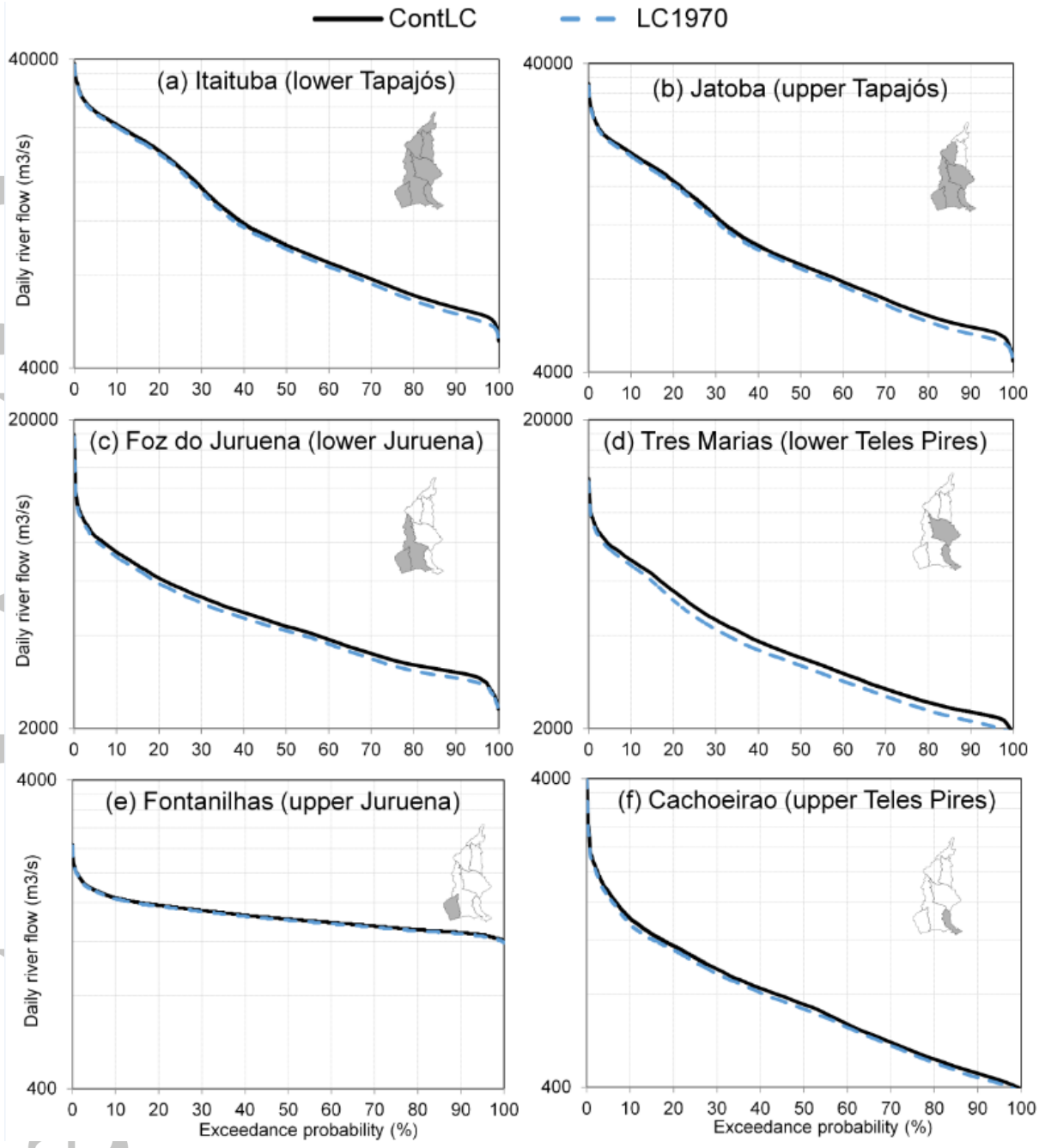

Figure 6. Flow duration curves for the period 1976-2008 comparing the probability distribution of daily flows for the two computer simulations. Effects of deforestation are most evident in stations in the middle of the basin (panels b, c, and d), and at each station the effects increased with exceedance probability.

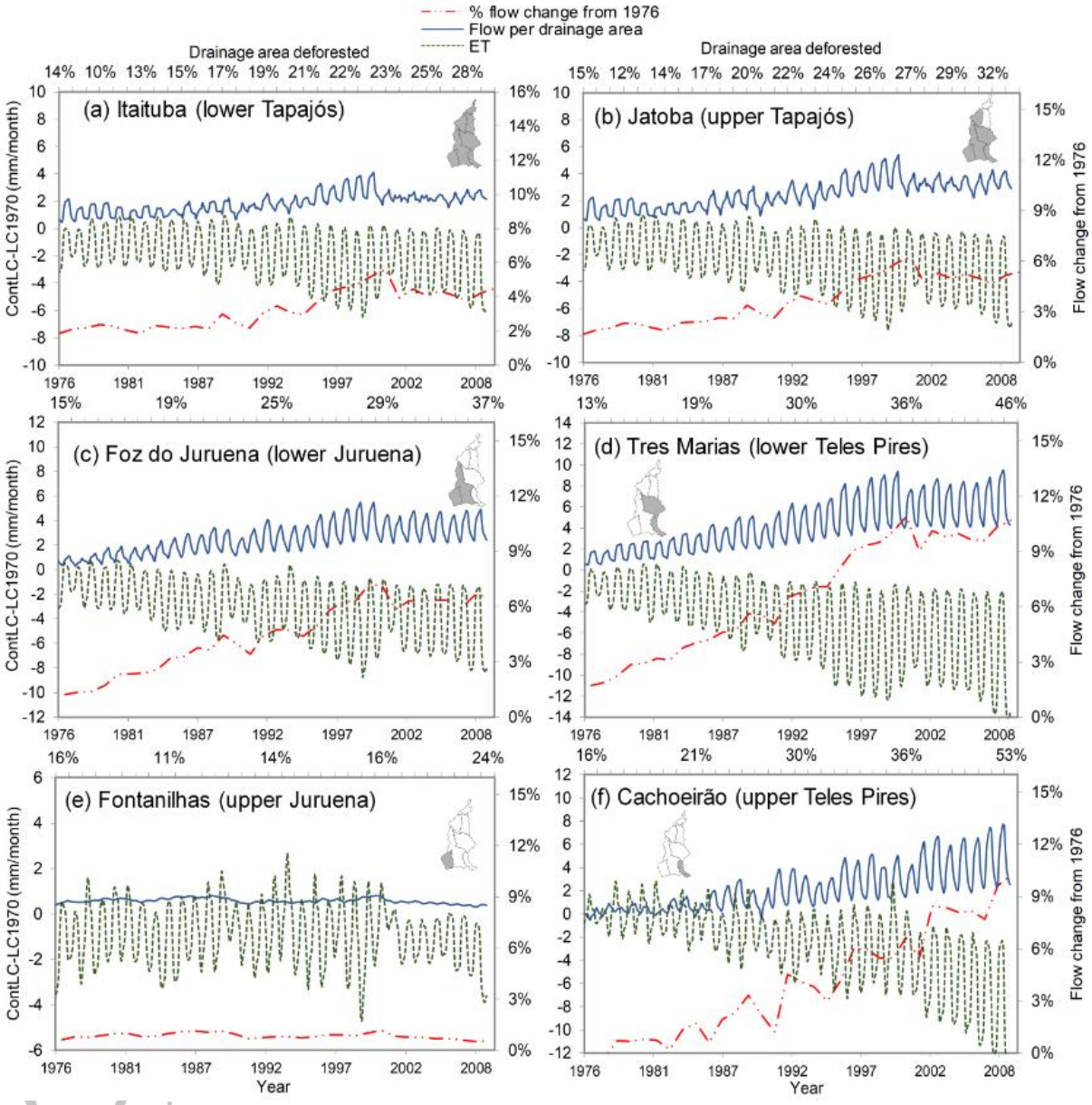

Figure 7. Time series of the arithmetic difference between results from simulations of climate with land cover transitions (ContLC) and climate effects alone (1970LC). The effects of deforestation on evapotranspiration (green dotted lines) and flow per drainage area (bold blue lines) are presented as 6-month running means in the left axis. The extent of the drainage area is marked in grey in the inserted basin map in each frame. Percent change in flow relative to 1976 conditions (dashed red line) is presented in the right axis.